



Contents lists available at ScienceDirect

Expert Systems with Applications

journal homepage: www.elsevier.com/locate/eswa

The mechanical assembly dimensional measurements with the automated visual inspection system

J. Rejc^{a,*}, F. Kovačič^b, A. Trpin^b, I. Turk^b, M. Štrus^b, D. Rejc^b, P. Obid^b, M. Munih^a

^a Faculty on Electrical Engineering, University of Ljubljana, Tržaška 25, 1000 Ljubljana, Slovenia

^b ETA Cerklno, Platiševa 39, 5282 Cerklno, Slovenia

ARTICLE INFO

Keywords:

Video camera
Lenses
Polynomial approximation
Protector
Non-contact dimensional measurements

ABSTRACT

This article describes the automated visual inspection system for dimensional measurements of a mechanical assembly, called the protector, where a USB video camera with regular lens is used. A special user software was written. It uses a linear and a polynomial approximation for defining edges of selected protector structures. A higher order polynomial approximation is also used for pixel to metric units transformation. The accuracy, the repeatability and especially the usability of automated visual inspection system was verified with protectors, previously measured with the reference measurement method. The verification procedure showed that the measurement accuracy is in the range of ± 0.02 mm. The time necessary for frame capturing, image processing and displaying the measurement results is less than a second. The comparison measurements showed that this system can not be used as a replacement for the current measurement system of monitoring switch-off temperatures in a oven. However, the presented visual inspection system can be used as a dimensional measurement and control system in the company testing laboratory.

© 2011 Elsevier Ltd. All rights reserved.

1. Introduction

The article describes the structure, the operation and the calibration of the automated visual inspection (AVI) system for dimensional measurements of assembly, called the protector (Fig. 1). The protector is a control and safety element, installed in cast-iron cooking plates of different sizes and nominal power. It has the task to switch-off the electrical power of the heating coils in the case of overheating.

Today many companies develop and install new instrumentation systems to improve the quality of their products, lower the false production quantities and to fulfill the international standards, such as ISO 9001. Among these systems are also the AVI systems, mainly used for part counting, location and shape recognition, for identification, sorting, measurement, testing and inspection purposes (Haralick & Shapiro, 1991).

The literature defines inspection as a procedure where AVI systems are used for determination of the product compliance with prescribed criterion (Newman & Jain, 1995). In inspection, a sensor for image sampling is used. The images are usually processed by video image processing methods. Such a system consolidate technology for material finishing, lightning, image sampling and computer hardware and software.

The AVI system applications can be placed in the following groups (Chin & Harlow, 1982; Dom et al., 1995; Don Braggins, xxxx): dimensional measurements, error detection, setting the object similarities and character recognition. In our project we combined the first two groups. The first group includes dimensional measurement with the non-contact acquisition of some dimensions between protector components. Before the measurements are performed, the tolerances must be provided (Griffin & Rene Villalobos, 1992). The second group is error detection on the manufactured products. The errors can appear as cracks, material structure irregularities and false assembly of the manufactured parts (Ravi-shankar Rao, 1996).

The AVI systems can be implemented in all manufacturing phases, from input inspection, manufacturing process and output control inspection (Batchelor & Whelan, 1996). In the group of the input inspection belongs an inspection of input materials. During this inspection, the material quality and suitability is verified. Today most AVI systems are set in the production phase, where the manufacturing quality is verified. In this phase it is possible to withdraw false products. This reflects in higher productivity, improved products quality, lower power and material consumption and more efficient production. In the output control the manufactured products are tested. This prevents selling false or low quality products. Our AVI system can be put in the second and the third phase.

The AVI systems have many advantages over human workers. A human can perform measurements much slower and less accurate

* Corresponding author. Tel.: +386 1 4768 379; fax: +386 1 4768 239.

E-mail address: jure.rejc@robo.fe.uni-lj.si (J. Rejc).

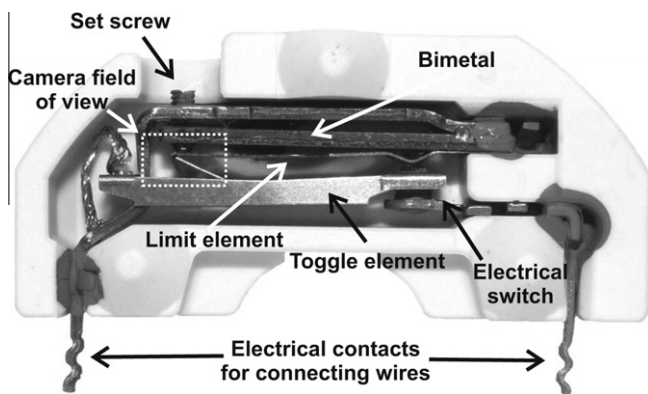


Fig. 1. Basic structure of the protector.

than AVI systems. In many cases the human measurement results are subjective and depend on workers's experience. Before the AVI system can replace the human worker it must be tested for accuracy and measurement errors. Measurement errors can occur because of the object translations regarding to the video camera, inappropriate optics, badly captured images and quantization.

The object translations towards the camera can result in a blurred image. Because the image sensor (e.g. CCD) is very small, a small translation of the object can result in a huge image blurring. This can be prevented with object stabilization during image capturing, as in our system. In case of system vibrations (Ho, 1983), the vibration isolators or the stroboscopic lightening can be used.

The errors that are a consequence of inappropriate optics can be mainly found as a zone error (spherical aberration). In this effect, the light rays close and parallel to the optical axis are intersected too far away from the lens. Contrary, if the rays run through the edge of the lens, they are intersected closer. In lens systems, the effect can be minimized using special combinations of convex and concave lenses, as well as using aspheric lenses. Beside this effect, astigmatism must also be mentioned. In astigmatism the set of rays, that emerge from one point out of optical axis, are copied into the set with elliptical shape. Also this effect can be minimized by the use of special lens systems. Literature (Yi-Chin et al., 2006) also refers to the color or chromatic error aberration caused by dispersion, because the lens for purple light has a shorter focal length than for the red color. The system of lenses also minimizes this error.

The image capturing means that the outer continuous world is digitalized and this process causes the quantization error. This is directly related to the image sensor resolution. Higher resolution means lower error, but higher image processing time. For this reason a compromise must be found to satisfy both criteria.

Using the thresholds to separate the objects from the background is extremely important, meaning that the image quality is high and the edges well expressed. For this reason it is necessary to choose the correct lighting. Literature states that a proper lighting design in machine vision is a complex process and depends on many factors. The rules can not be given, only the guidance (Taranis, Allen, & Tsai, 1995; Murase & Nayar, 1994). When the lighting is planned, the constructor should consider the use of various types of illumination (monochromatic, polarized, focused, diffuse) and various properties of observed objects: diffusion, reflectivity, translucency and transparency. In addition, it is possible to light the object in many ways (Miller & Friedman, 2003) and each has its advantages and disadvantages. Also here the universal rule does not exist: from the front, rear, with the polarized or non-polarized light, direct light, with structured and stroboscopic light.

In the work described in this article, we have exploited the pool of published knowledge, utilized low price hardware, developed

specific software for image acquisition and dimensional measurements of the mechanical assembly and established measuring accuracy, repeatability and suitability of the system.

2. Protector

The basic components of the protector (Fig. 1) are electrical contacts for connecting wires, electrical switch, bimetal with the set screw, limit and toggle element. In protector, the bimetal bends and over the set screw exerts force on the limit element. When the limit element is pressed enough, it triggers the toggle element, which represents half of the electrical switch.

The AVI system was developed for a particular protector type. It has nominal switch-off temperature at 400 °C with tolerances of ± 30 °C. In order to achieve switching within the prescribed temperatures, the most important is the distance between the toggle element and the limit element, marked with the letter A (Fig. 7). Fine adjustment of this distance is performed with the configuration machines, where first the set screw is set in a way that the protector switches-off at room temperature. Switching event is checked through electrical contacts. Since it is practically impossible and economically completely unjustified to adjust the set screw at the rated temperature (400 °C), the set screw is spined at room temperature for a certain angle in reverse and fixated with glue. This new distance A should be an appropriate distance for protector to switch-off at the rated temperature.

The described procedure is carried out on all manufactured protectors. Verification of correctness of the screw-set distance is done statistically in the production in special ovens, where the switch-off temperatures are verified at high temperatures. These measured switch-off temperatures are used to set the proper number of reverse revolutions of the set screw during production. An identical oven is also used in laboratory and is described later.

The control, whether the protector system is correctly assembled, is now visually performed by the worker, which causes a possibility of subjective evaluation. Therefore, there may be some false assembled protectors compound in the cooking plate. As a consequence, there is a need for introducing the AVI system, which would eliminate the false protectors and possibly set the appropriate distance A. In addition, the measurement of other dimensions, prescribed by tolerances, can be done. These measurement results can be statistically observed in a long time period.

3. Automated visual inspection system

The decision to develop a system for non-contact visual system was only acceptable, due to the structure and composition of individual protector parts (Sato, Ishikawa, Hiraki, & Takamasu, 2002). In the class of non-contact measuring sensors are widely used triangulation laser systems (Nguyen, 1995), that project laser light as dot, line or other curve. Test trials of measurement by laser triangulation line system Keyence LJ-G030 have shown, that the desired dimensions of components and the distances between them can not be measured, due to too small distances between the components of the protector.

Also in video systems many problems are found. From the hardware, video camera types, lens choice and particularly the correct lighting. In measuring systems it is also very important to have the proper camera field of view, which is inversely related to the measurement accuracy, that is exhaustively discussed by Hsua, Lina, and Lee (2005).

The developed AVI system for measuring the dimensions and distances between certain components of the protector is shown in Fig. 2. It consists of a monochromatic video camera, a lens with appropriate extension rings, an adequate lighting and a mechanical

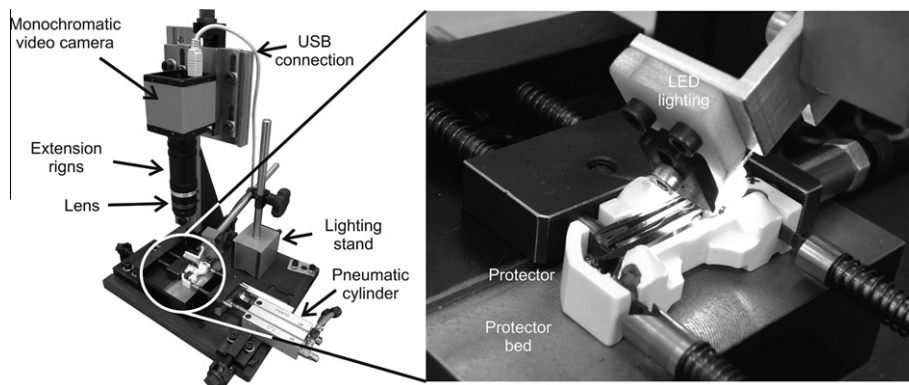


Fig. 2. Prototype of AVI system with close-up showing lighting solution and protector bed.

clamping system with a light shield and a protector positioning system.

3.1. Video camera

When the video camera needs to be selected, the following factors have to be accounted (Davies, 2005): what kind of image we want to capture, line or matrix; do we need black and white or color sensor; which image resolution is the most suitable for desired properties and how the object is illuminated.

Our customer defined a measurement error within the range of ± 0.01 mm and field of view to be about 5×3 mm ($W \times H$). To achieve the desired measurement error the recommended resolution of the measuring system is at least ten times lower, in our case $1 \mu\text{m}$. The customer required in the first stage a prototype system. For this reason a compromise in the initial financial investment was needed. Selected and installed monochrome camera was DMK 41AU02 type, produced by The Imaging Source. It has a Sony CCD array image sensor size $1/2''$ with a resolution of 1280×960 pixels. In this way we achieved a horizontal resolution of approximately $4 \mu\text{m}$ on the image element and vertically approximately $3 \mu\text{m}$ on the image element. The camera is connected to a PC via USB 2.0 connection.

3.2. Mechanical structure with a light shield

The base of the prototype system is a mechanical structure, as shown in Fig. 2. The figure presents the system without a light shield, which is necessary to maintain constant lighting conditions. The framework structure is designed for a rigid attachment of the video camera. The camera attachment system allows positioning of the camera in all three axes of the Cartesian coordinate system. This is done by special screws. The system is designed in a way, that the camera is mounted on a special groove to set camera field of view perpendicularly to the protector bed. This is extremely important for the image depth of field.

In addition, the mechanical structure has also a function to properly position the protector (2) in camera field of view, as can be seen on Fig. 3. The user can roughly position the protector in the prototype system. Then, the protector is pushed (1) with a pneumatic cylinder to predetermined limit position (4), all this enables a narrower camera field of view. The design of the guides (5) was very careful. It was necessary to lean the guides on the protector switch system to position protectors the same way according to the camera field of view. This is a must due to large tolerances of the ceramic housing. In the direction where the camera's field of view is larger, a support (3) was made directly on the ceramic body of the protector, which has proved quite appropriate. This support

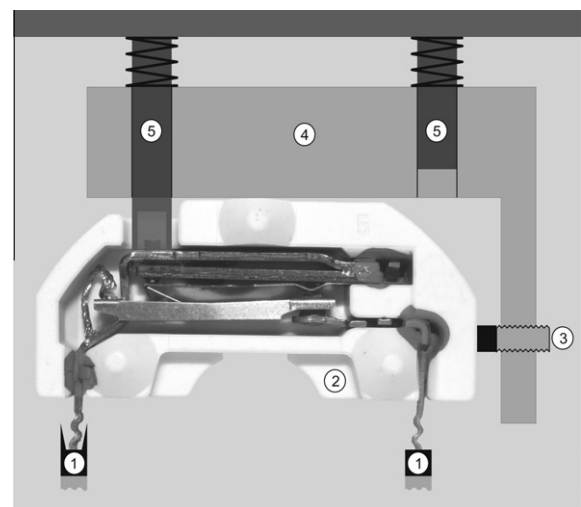


Fig. 3. Protector positioning in AVI system.

was made with a screw, the other two lean points are using springs.

3.3. The lens and the extension rings

The most important component of each video system is an adequate lens. Similarly to the camera, cheaper optics were chosen, from the company Fujinon, type HF50HA-1B, the C mount adapter. In order to minimize the distortion, the lens has a focal length of 50 mm, the minimal working distance is 0.5 m. The lens allows manual focusing and shutter adjustment from F2.3 to F22.

Since the selected lens has a large focal length, the depth of field was lost, which decreases with the square of focal length (Eq. (1)). In this equation abbreviation WD stands for working distance, BS is a blur spot, I represents the iris, while F is the focal length. During the later trials, the reduction of depth of field, has not been a problem. Otherwise, the lens with a smaller focal length should have been mounted. However the use of such lens would result in greater image distortion.

$$\text{DOF} = \frac{\text{WD}}{1 \pm \text{BS} \cdot I \cdot \frac{\text{WD}-F}{F^2}} \quad (1)$$

The desired field of view on the protector was very small and the lens minimum working distance was too large. These reasons required installation of the extension rings, between the camera mount and the lens. With these rings, the lens was moved away

from the camera for 65 mm (5 + 10 + 10 + 40 mm). This way was reduced the field of view to about 5×3 mm ($W \times H$) and also reduced the minimum working distance to 11 cm.

3.4. The lighting

The object in the presented system would be lighted best from the back with a diffused light. However, this lighting could not be implemented, due to the protector closure on all sides, except from the camera direction.

The tests proved that the most appropriate lighting is the use of two white LEDs, as shown in Fig. 4. If single LED is used, then adequate illumination of the background ceramic could not be achieved. The diodes are the most appropriate cold sources, because the protector should not be heated and possibly bending the bimetal. Diodes have a diameter of 5 mm, mounted side by side in a plastic holder with a thickness of 5 mm. The holder is fixed to the magnetic stand, used for defining lighting conditions.

The beam-width of the diode is 15° , the intensity is 8000–11000 mcd (milli-candelas) at initial current of 20 mA. The diode supply voltage was 5 V through the USB computer port, with the current restricted by 67Ω resistor. For the proper protector illumination conditions, the angle α , between the plastic holder and the ground, must be between 55° and 60° . This angle range enables the illumination of the protector background ceramic homogeneously, as in the case with the diffuse illumination being used.

To prevent the illumination of upper metal parts of the protector switch system, a special black curtain is installed over the LED's diameter, as is seen in Fig. 4. Without this curtain the image contrast would not be satisfactory. This curtain blocks the half of the LED's diameter, but the amount of blocking range can be reduced to get wider illumination field. Besides the definition of angle α also dimension H and L were defined.

4. Software

4.1. User environment

For the AVI system a special software, following definitions of the customers, was prepared. They defined to use the prototype system as a parallel system in statistical control of the protectors in their laboratory. Statistical control is carried out in a special oven, where a series of protectors is manually inserted. These protectors are electrically connected to the computer system, which measures the switch-off temperature of each inserted protector.

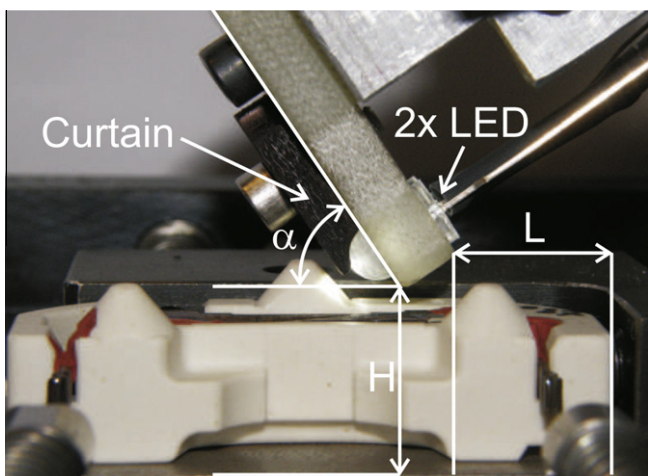


Fig. 4. Lighting solution.

The software is written in the Borland development environment C++ Builder 2006 for Microsoft Windows. To read the tolerance data of measured protector and saving the measured dimensions, a database Microsoft Access 2002 is used. The software communicates with the database via ODBC interface. To capture and play live image from the camera, which is connected to the PC via USB, the ActiveX components of the software IC Imaging Control 3.0, manufactured by company The Imaging Source, is used. For some image processing operations, were used functions from OpenCV open source package, version 1.1. In addition many applied functions were written in house. To position the protector in the mechanical bed, a pneumatic cylinder is used. It is activated through the electro-pneumatic valve and PC parallel port.

The user interface (Fig. 5) gives a live grayscale image that is outlined by the measured dimensions and binary image used to measure the dimensions. At the beginning of a new series of measurements, the user selects from the menu the appropriate protector type, sets the date and manufacturing batch, which represents the head of the measurements data. Then the protector should be inserted in bed in the numbered order, such as in the laboratory oven. Then the measurements should be manually initiated.

The program measures 5 dimensions. At the end of measurement the program informs the user with the results and about compliance with the tolerances. All data is saved in a database. The program allows setting the relevant tolerances, usually only dimensions A and D (Fig. 7).

4.2. Image processing and dimensions calculation

Fig. 6 shows a flow diagram of the developed program. The application first, via the parallel port, sets the logic level on pin 2 high, afterwards amplified to 24 V. This 24 V controls the electro-pneumatic valve which controls the pneumatic cylinder actuator for proper protector positioning.

To detect edges of the objects in the image, it is converted to a binary image. This is accomplished by using the threshold. The threshold value is defined by the user in advance through the appropriate menu in the program. This value is then used for system calibration and measurement mode. After the image is binarized the program checks the image's adequacy. The procedure first checks if the lens is covered by comparing the percentage of the black and white pixels. In the similar way it is checked if a protector is present in the image. If it is not, the image is completely white.

The first steps in determining the protector dimensions is the search for the left vertical edge, which is on Figs. 6 and 7 marked with the number 1. Search takes place within the square, which is clearly visible on the left side of the Fig. 7. The program initially

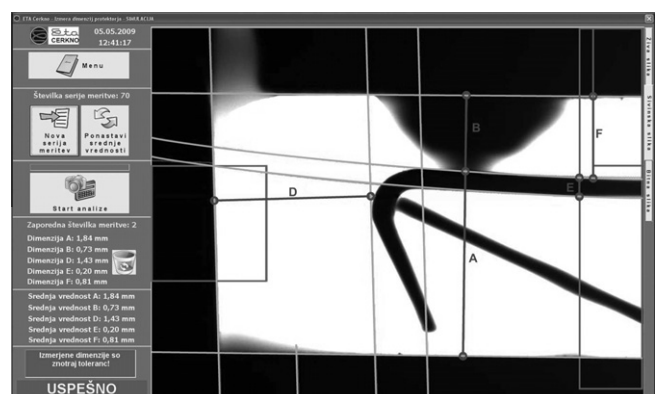


Fig. 5. User interface.

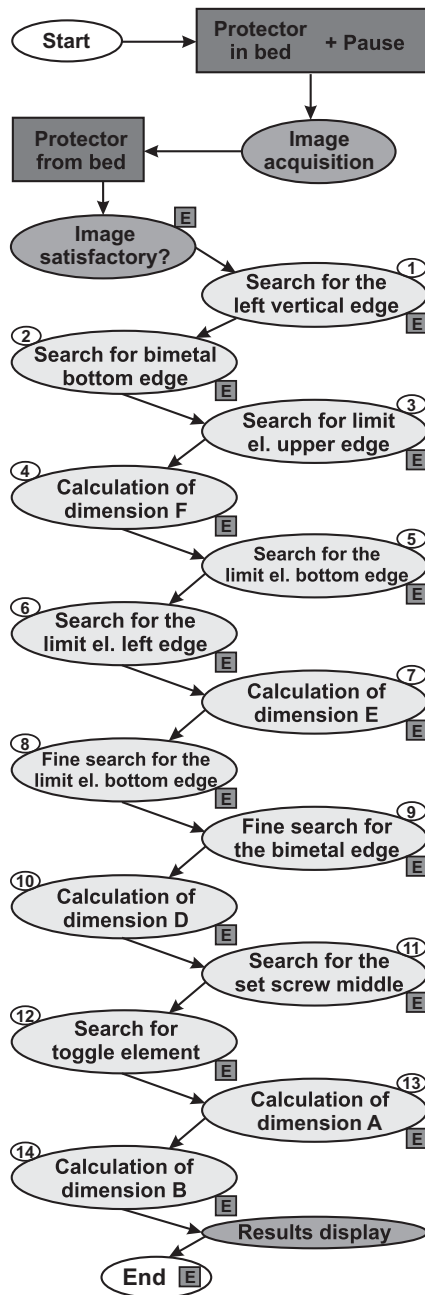


Fig. 6. Software flow diagram.

checks if all left area in the square is black. If not, an error is returned and the measurement procedure is stopped. Determination of the left vertical edge proceeds by finding the edge on the binary image. Then the method of the least squares (Eqs. (2) and (3)) is used, through the stored coordinates of the edge points. The polynomial of 1st order that is equal to the linear line is approximated through the binary edge points (Eq. (4)). This method is used for all edge approximations, both for linear and higher order polynomial approximations. The procedure filters the edges, which is important due to small dust particles that can appear on edges. When using mathematical equations also the distance calculations are more accurate. In the case that error occurs during the mathematical edge approximation, the program informs the user and procedure is terminated. On the diagram such an event is marked with the letter E.

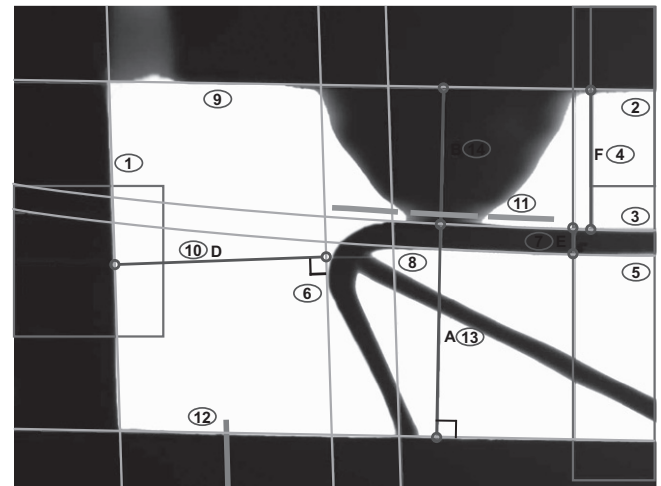


Fig. 7. Search areas and measured dimensions.

$$A = [1, x, x^2, \dots, x^n], \tag{2}$$

$$p = [A^T \cdot A]^{-1} \cdot A^T \cdot y, \tag{3}$$

$$\hat{y} = p_0 + p_1 \cdot x + p_2 \cdot x^2 + \dots + p_n \cdot x^n. \tag{4}$$

The same sequence is repeated in the case of the bimetal edge, marked with number 2. Searching procedure is in the extreme upper right area of the image in the rectangle whose position is also predefined by the user. In this area another user predefined rectangle is present and used for finding the upper edge of the limit element, marked with the number 3. The next event mathematically describes both, the edge of the bimetal and the upper edge of the limit element (numbers 2 and 3). With this information a distance between these two lines is calculated, on the Fig. 7 marked with a letter F and on the Fig. 6 with a step number 4. The calculation of the distance F is needed to recognize possible deviations that suggest poorly configured protectors. In this case no further analysis is required and the program terminates.

All the required distances are calculated by defining the intersection points between mathematically approximated lines and then by Eq. (5) the distances between these points are calculated:

$$d(A, B) = \sqrt{(x_2 - x_1)^2 + (y_2 - y_1)^2}, \tag{5}$$

In Fig. 6 number 5 shows a step in which the lower edge of the limit element is found and mathematically approximated by the linear line. This procedure is performed on the right side of the image, still within the specified rectangle. By setting this line, the limit element thickness is calculated, marked with the letter E and number 7 in Fig. 7. The tests showed that measurements of dimension E are not as accurate as we wanted, as a consequence of the limit element material reflectivity. This reason can cause the thickness of the limit element to be too small, up to 0.02 mm comparing to the manufactured dimension. The limit element material is manufactured by the EN ISO 9445: 2006 (International Standard ISO, 2006) standard, class P. This standard defines limit element thickness of 0.200 ± 0.008 mm. Due to the standard's very narrow tolerances, in the further calculations a value of 0.20 mm is used.

In the next step, based on the defined edges, the left edge or a hook of the limit element is defined. In the utmost point of the hook the vertical line from step 1 is applied again. This line is marked with the number 6. In the middle of these two parallel lines, the perpendicular distance D is calculated, on Figs. 6 and 7 marked with line number 10. In the design drawings for protector

this distance is defined as 1.6 ± 0.05 mm. It directly influences the force of bimetal pushing the toggle element.

Due to the force exerted on the limit element, it slightly bends and linear approximation of the upper edge is not suitable. Fig. 7 demonstrates that the upper edge of the limit element lies on the boundary where dimensions A and B connect. Therefore the definition of the boundary point is not possible. That is why the bottom limit element edge is mathematically defined, by using 2nd order polynomial, marked with the line number 8. As next, this mathematically approximated polynomial is shifted upwards for the fixed dimension E . This line represents the upper edge of the limit element.

Tests uncovered that the setting of the bimetal edge, marked with the line number 2, is in most cases satisfactory only when the field of search rectangle is positioned upper-right. Therefore, we were forced to define the bimetal edge also on the left side of the set-screw, which is represented as line number 9. This search procedure is relative to the vertical line that defines the left edge of the limit element hook and carried out in preset width. By combining data of the bimetal edge from Section 2 and 9, the bimetal bottom edge is most precisely defined.

The calculations of the dimensions A and B are carried out in the contact point of the set screw and the limit element. Since this point depends on the position of the set screw, it is impossible to determine this point precisely. Most reasonable is that the point of contact between the set screw and the limit element is taken in the middle of the set screw, as is defined in section 11. The middle point definition procedure uses the area from nearby right side of the limit element hook vertical line and left rectangle side for limit element edge search, letter E or line number 7. At this step the polynomial approximation of the upper limit element edge is shifted upwards for 0.04 mm. The algorithm first finds the black area of the set screw, the middle region represents the middle of the set-screw. Using this procedure the middle line of the set screw can not be defined highly precise, but the tests demonstrated that the approach gives satisfactory results.

A huge challenge was to define the toggle element edge, in Fig. 7 numbered with line 12. Finding that edge was not trivial due to the shadows that can occasionally appear in the left bottom area of the image. These shadows can appear from the limit element hook blocking the light. For successful definition of the toggle element edge, a special algorithm was created. The algorithm is based on setting the dynamic threshold of the image between the two preset thresholds. These two limits are set by the user, usually between 10 and 100, with the lower and upper limits being 0 and 255. The dynamic adjustment step is 5. This dynamic approach was chosen to select optimal value, i.e. when the threshold is increased the shadow slowly appears. The tests showed that there is a small white area between the shadow and the toggle element edge, which is getting smaller with higher threshold values. When the threshold is high enough the white area disappears. This threshold is too high, thus previous value is used. Next, the mathematical approximation of the edge is carried out. The search is started from the short vertical line number 12 to the extreme right edge of the image, from bottom up. The last black pixel represents the eventual edge point. In this area dirt, shadows and part of the limit element hook can occur. That is why a moving average algorithm over the found edge points is used. This means that over the edge points a virtual window shifts from left to right, the step size is a pixel value. If the edge point in a window is too far away from the last local mean value, then this point gets the mean value. This algorithm does not catch the influence of far away points as in the case of direct use of the least mean square method. Over the pool of edge binary points a linear approximation is defined, describing the toggle element edge.

The last approximation line enables the calculation of dimensions A and B , in Figs. 6 in Fig. 7 marked as lines number 13 and

14. The calculation is performed by setting a line through the middle of the set screw perpendicular to the toggle element edge line. The intersections of approximated lines represent the dimensions A and B .

When the analysis is finished, the user is informed about the measurement results and the program window displays dimensions A, B, D, E and F . The user is also informed whether the dimensions are in the predefined boundaries or not and the data is saved in the database.

4.3. Calibration of the AVI system

Every measuring instrument has to be calibrated before the use. For this purpose, our software offers also the calibration of the measuring AVI system. For calibration purposes the user uses three calibration protectors, with known dimensions A, B and E , in our case previously measured with the certified profile projector measuring system, type Mitutoyo PV500.

The user has to manually insert the pre-measured dimension values in the empty software fields, before the first calibration. The calibration procedure is the same as the measuring procedure, described in previous section. The main difference in calibration procedure is that dimensions are not calculated, but rather the number of pixels between intersection lines is defined. The number of pixels between these edges is a decimal value number.

By using the decimal pixel values the transformation between number of pixels to metric units is performed. Because the optics nonlinearities, the relationship between the pixels is not completely linear. For this reason the user can select which approximation polynomial order best transforms the number of pixels into metric units. The polynomial order can be selected from 1 to 6. This polynomial transformation is calculated by using the residuals and the factor R^2 , called the coefficient of determination. This coefficient has a value between 0 and 1, where higher value reflects better approximation. An example of the transformation approximation can be seen on Fig. 8, where polynomial of 4th order is used.

R^2 was calculated using Eq. (6), where y is the measured value, \bar{y} is the mean and \hat{y} is the current calculated polynomial value.

$$\begin{aligned} \text{ResidualSS} &= \sum (y - \hat{y})^2, \\ \text{TotalSS} &= \sum (y - \bar{y})^2, \\ R^2 &= 1 - \frac{\text{ResidualSS}}{\text{TotalSS}}, \end{aligned} \quad (6)$$

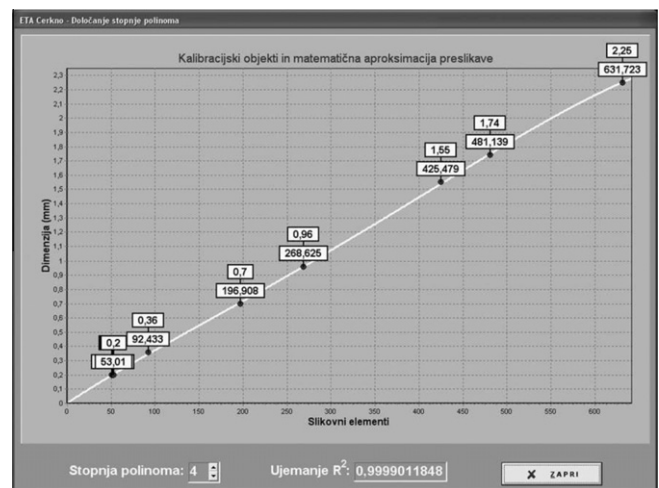


Fig. 8. User window for polynomial transformation from number of pixels into metric units.

For calibration purposes three normal protectors were chosen with dimensions A , B and E being the most spread over the AVI system measuring range. At this point it must be stated that also during the calibration procedure, the dimension E was fixed at value 0.20 mm. This value is the same as measured by using calibrated profile projector measuring system.

5. Methodology

5.1. Dimensional measurements of the calibration protectors

For the calibration of the presented AVI system three objects are needed. Their known dimensions A , B and E are pre-measured with an optical profile projector. It was also used to measure another five protectors used as control samples for defining the measurement error.

On these eight protectors dimensions A , B and E were measured. Measurements were performed by the use of the profile projector, type Mitutoyo PV500. The resolution of this system is 1 μm with the repeatability of 3 μm . The magnifying factor during the measurements was set to 20 \times . For more accurate protector positioning on the measurement board also a special magnifying glass with a magnifying factor of 10 \times was applied. Measurement uncertainty of the profile projector is described by the publication EA-4/02 (European Co-operation for Accreditation, 1999) and Eq. (7). The result and the measured distance L is expressed in μm .

$$u = \pm(4 + 5 \cdot 10^{-6} \cdot L), \quad (7)$$

Calibration of the profile projector measuring system is performed every 2 years. For the calibration special calibrating blocks and glass rulers are used. The procedure for the calibration of the profile projector measuring system is not defined in detail by any international standard. Therefore the calibration is performed by internal calibration procedures, which are accredited by an external judge. In our case, by the Dutch independent, internationally recognized testing and certification institute, called NMI (Nederlands Meetinstituut). Every calibration protector was measured only once at room temperature (23 ± 1) $^{\circ}\text{C}$.

The measurement procedure is as following. The calibration protector is laid on the glass surface of the profile projector. The profile projector measuring system, by the use of lenses and mirrors, projects the image of the measured object on the glass surface equipped with coordinate system and ruler marks. By rotating the micrometers the coordinate system is moved to the preferred position and orientation. In our case the X axis was levelled to the toggle element and the Y axis to the middle of the set screw. After levelling, the coordinate system was positioned at the bottom of the limit element still in the middle of the set screw. This was the position where the micrometers values were reset to zero. This center point was chosen as the most exposed part of the protector when measured by a profile projector. The position of this center point is not appropriate for measuring distances A and B , because the distance A is too short and distance B too long for 0.20 mm, as is the thickness of limit element material.

This measurement procedure has a great subjective influence of the person who performs the measurements, because many edges are difficult to define with great precision, although the use of magnification helps to achieve more accurate measurements.

From all 8 reference protectors, three were defined as calibration objects to define the transformation of the number of pixels into metric units, in our case in millimeters. To describe the transformation a polynomial transformation of the 4th order was used alongside the linear transformation function. The 4th order polynomial had the highest R^2 value. The calibration protectors with sequence numbers 2, 6 and 7 had their measured values A , B and E

the most spread over the field of view of the AVI system. Other protectors, numbers 1, 3, 4, 5 and 8, had been used as control objects for defining measurement accuracy and repeatability of the AVI system. The measurements with the AVI system were performed at room temperature of 23 $^{\circ}\text{C}$. Every protector was manually positioned into the system bed. After a measurement was run, every protector was manually removed from the system bed. Number of repeated measurements on each protector was 25.

5.2. Dimensional measurements of the protectors

To ensure that the manufactured protectors switch-off at the right temperatures, it is necessary to statistically test protectors in a laboratory. 72 protectors randomly taken from already sealed packages presents a measurement set. Several sets are tested daily. Each protectors set is put into a special oven. Every protector in the oven is electrically connected to observe the state of the switch. The oven is gradually heated. The inner temperature is measured with a PT-100 class A temperature sensor. Its measurement error is expressed by Eq. (8). The calculation temperature (T_x) is at 400 $^{\circ}\text{C}$.

$$\Delta T = \pm(0.15 + 0.002 \cdot T_x) = \pm 0.95 \text{ }^{\circ}\text{C}. \quad (8)$$

The heating of the oven proceeds until the last protector reaches its switch-off temperature. For safety reasons the maximum inner temperature is set to 480 $^{\circ}\text{C}$, where the heaters are also switched off. After heating, the oven is passively cooled to the temperature where the last protector switches back on. The switch-off and switch-on temperature value of each protector are saved into a computer database. The procedure is repeated three times in the laboratory. As a measurement result, the average value of the second and the third cycle is used. This measurement procedure in a laboratory is very slow and every set takes 6–9 h to complete. In production facilities this slow procedure is performed only once.

This is the main reason why a faster measurement would be very welcome. The fastest method would be if the switch-off temperature is in correlation to the dimension A . The presented AVI system needs less than a second to assess the dimensions A , B , D and F . Including the protector manipulation, the overall time is less than 2 s, which is much less than manufacturing time cycle. Fast measurements using such a system would result in testing of each manufactured protector, as opposed to today's statistical sampling methods.

Until today no comparative measurement on a large set of protectors was performed, where the dimension A could be directly compared to the switch-off temperature. For measurement purposes a set of 220 protectors was chosen. All were fine calibrated during their production. Furthermore, a second set of 220 protectors was also chosen. They were only roughly calibrated at the set screw assembling. These are meant as non-calibrated. The reason to include also non-calibrated protectors, was to verify if only rough calibration was enough for production. All protectors were numbered and than measured by the presented AVI system and also with the reference heat and cool oven procedure. During measurements with the AVI system each protector was measured only once. In the oven the standard procedure was repeated. In the set of calibrated protectors 218 of them were successfully measured by the AVI system and 217 of the non-calibrated set. The reason why some of the protectors were not successfully measured originates from mechanical problems of the pneumatic positioning system of the AVI system. Some of the ceramic protector housings were out of tolerances.

6. Results

6.1. Dimensional measurements of the calibration protectors

The measurement results of dimensions A , B and E obtained when using a certified profile projector are given in Table 1. All

Table 1
Reference dimensions A and B.

Protector dimension	1 (mm)	2 (mm)	3 (mm)	4 (mm)
A	1.87	1.56	1.80	1.57
B	0.71	0.95	0.70	1.09
Protector	5	6	7	8
A	1.76	1.76	2.27	1.32
B	0.87	0.71	0.35	1.29

measurements are rounded to two decimal places, the third does not represent measurement accuracy. The dimension *E* is 0.20 mm. The other two dimensions are widely spread over the measuring range. The range of dimension *A* ranges from 1.32 to 2.27 mm, resulting in 0.95 mm dispersion. The spread of the dimension *B* is 0.94 mm wide, from 0.35 to 1.29 mm. The sum of both dimensions is 2.55 mm, representing almost whole vertical range of the camera field of view, which is approximately 3 mm.

The results gathered by AVI system with the linear transformation between number of pixels and metric units are displayed in Table 2. The first column lists the number of the measured protector, the second shows measured dimension, the third contains mean measured distances, the fourth the error between current mean and reference value, which can represent the accuracy and the last column the error between current mean value and measured value. The last can be considered as measurement repeatability.

The errors measured in the calibration protectors (numbered 2, 6 and 7) are in the range of ± 0.02 mm, meaning around ± 5 pixels. If the repeatability is observed the values range from 0.00 to 0.01 mm, meaning around 2 pixels.

Looking at the other five protectors, the errors are in the same range of ± 0.02 mm as in calibration protectors. The repeatability value of these protectors is ± 0.01 mm and as such completely satisfactory.

The results measured by AVI system with the 4th order polynomial interpolation between number of pixels and metric units, are displayed in Table 3. This polynomial order demonstrated the highest R^2 value. As before, the first column shows the number of the measured protector, the second lists dimension abbreviation, the third brings mean measured distances, the fourth the error between mean and reference value, which can represent the accuracy and the last column the error between mean value and measured value. The last column can be considered as a measurement repeatability.

Table 2
Measurement results when using linear transformation.

No.	Dimension	Mean value (mm)	Error (mm)	Repeatability (mm)	
				Min	Max
2	A	1.54	0.02	0.00	0.00
	B	0.97	-0.02	0.00	0.00
6	A	1.75	0.01	0.00	0.00
	B	0.71	0.00	0.00	0.01
7	A	2.29	-0.02	0.00	0.01
	B	0.34	0.01	0.00	0.01
1	A	1.87	0.00	0.00	0.00
	B	0.71	0.00	0.00	0.01
3	A	1.81	-0.01	-0.01	0.00
	B	0.70	0.00	0.00	0.00
4	A	1.55	0.02	-0.01	0.01
	B	1.09	0.00	0.00	0.00
5	A	1.77	-0.01	-0.02	0.00
	B	0.86	0.01	0.00	0.00
8	A	1.30	0.02	0.00	0.00
	B	1.29	0.00	-0.01	0.00

Table 3
Measuring results when using 4th order polynomial transformation.

No.	Dimension	Mean value (mm)	Error (mm)	Repeatability (mm)	
				Min	Max
2	A	1.56	0.00	-0.01	0.00
	B	0.96	-0.01	-0.01	0.00
6	A	1.77	-0.01	-0.01	0.00
	B	0.70	0.01	-0.01	0.00
7	A	2.28	-0.01	-0.01	0.00
	B	0.34	0.01	-0.01	0.00
1	A	1.90	-0.03	-0.01	0.00
	B	0.69	0.02	0.00	0.01
3	A	1.84	-0.04	-0.01	0.00
	B	0.68	0.00	0.00	0.00
4	A	1.57	0.00	-0.01	0.01
	B	1.09	0.00	-0.01	0.00
5	A	1.80	-0.04	-0.01	0.00
	B	0.84	0.03	0.00	0.01
8	A	1.30	0.02	0.00	0.01
	B	1.29	0.00	0.00	0.00

The error measured in the calibration protectors (numbered 2, 6 and 7) is in the range of ± 0.01 mm, meaning around ± 2 pixels. The repeatability values range from -0.01 to 0.00 mm.

When checking the other five protectors, the encountered errors are much higher. In protectors 3 and 5 the error for dimension *A* is -0.04 mm, in dimension *B* the error is smaller having a value of 0.02 mm. The repeatability is in range from -0.02 to 0.01 mm.

Fig. 9 shows errors between results measured by the AVI system and the reference values measured with the profile projector. The bars for dimensions *A* and *B* are displayed for 1st (linear) and 4th order polynomials used to transform number of pixels to metric units. The upper diagram shows comparison for dimension *A* and the bottom for dimension *B*. The horizontal axis represents the protector number and the vertical axis the error in millimeters. Again it can be seen that error is more equally distributed over the measuring range in the case of linear transformation.

6.2. Dimensional measurements of the protectors

In Fig. 10, a histogram shows switch-off temperatures of 220 calibrated protectors from the production, without using AVI system. The measurement tests were made in a laboratory oven.

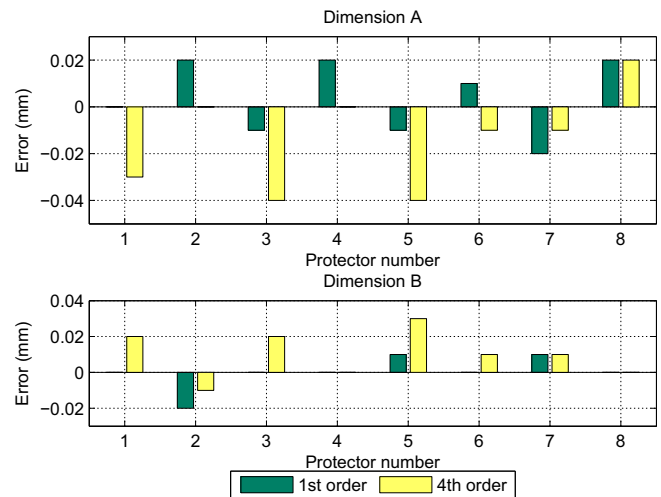


Fig. 9. The error according to the polynomial order; the profile projector values are taken as standard.

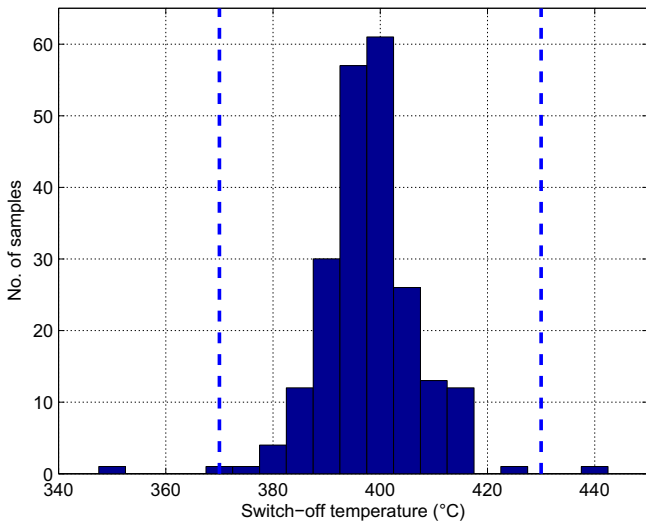


Fig. 10. Sample of 220 calibrated protectors; switch-off temperature.

The horizontal axis shows switch-off temperatures in degrees Celsius, steps of 20 °C. Two vertical dashed lines represent the tolerance area of ± 30 °C, according to predefined switch-off temperature of 400 °C. The mean value of measured sample is 398 °C and standard deviation 9.2 °C. These results show that the majority of protectors switch-off in the tolerance range. Only three protectors switched-off outside the tolerance area, with switch-off temperatures: 352, 369 and 441 °C.

The measurements of the switch-off temperatures of protectors calibrated in production demonstrated that they are in most cases properly calibrated. For this reason the mean value of the dimension A can represent the mean switch-off temperature. The distribution of dimension A, measured with AVI system in observed sample is shown in Fig. 11. The mean value is 1.93 mm with standard deviation 0.05 mm. Based on these values the tolerance range was set to embrace equal number of protectors as seen in the tolerance area of switch-off temperatures. This way the set tolerance area has a width of ± 0.15 mm according to the mean value, on the figure being represented by two vertical dashed lines.

To replace the very slow measurements of the switch-off temperature in the oven with the AVI system approach, the relation

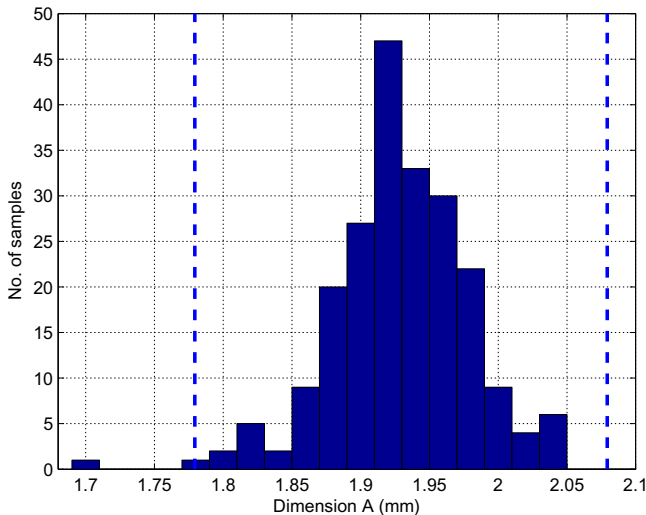


Fig. 11. Sample of 218 calibrated protectors; measurements of dimension A.

between dimension A and switch-off temperature should be linear (Fig. 12). The horizontal axis represents dimension A, the vertical axis stands for switch-off temperature in degrees Celsius. Each circle represents one numbered protector, the dashed lines define tolerance areas. If the relation would be linear, then the circles would appear on the line between the intersection of dashed lines. In the diagram it is clearly seen that the relation is not linear and too spread around the line. Furthermore, one protector with dimension A within the tolerance area switched-off at to high temperature.

The oven measurement results of switch-off temperatures for 220 non-calibrated protectors are shown in Fig. 13. The horizontal axis shows switch-off temperatures in degrees Celsius, step is 10 °C. Two vertical dashed lines represent previously used tolerance area of ± 30 °C, with desired switch-off temperature of 400 °C. The mean value for the sample is much higher, 425 °C with standard deviation 23.1 °C. According to these figures most protectors switch-off outside the tolerance range. 96 protectors had the switch-off temperatures higher than the maximal temperature in the oven that is 480 °C and are not included in Fig. 13.

The measurement results of dimension A by using AVI system for non-calibrated protectors are shown as histogram on Fig. 14.

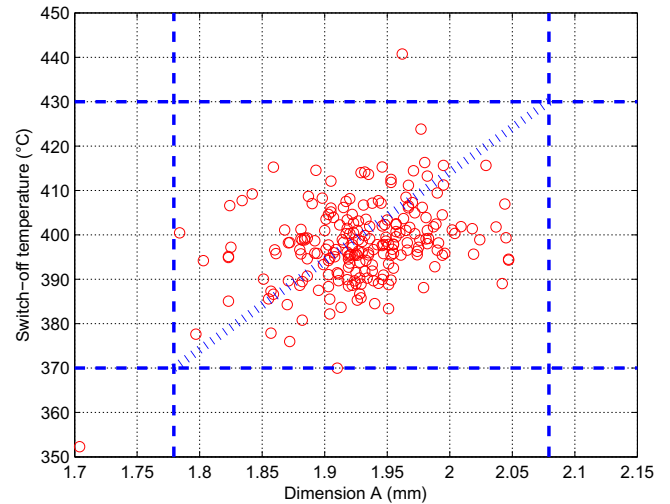


Fig. 12. Sample of 218 calibrated protectors: measured dimension A vs. switch-off temperature.

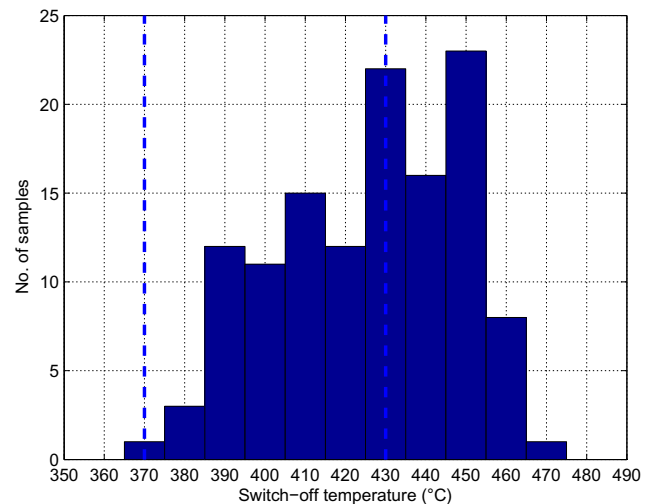


Fig. 13. Sample of 220 non-calibrated protectors; switch-off temperature.

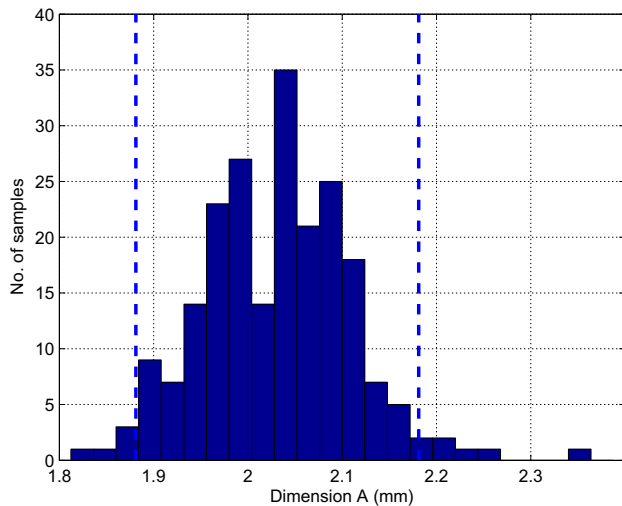


Fig. 14. Sample of 217 non-calibrated protectors; measurements of dimension A.

The mean value of distance A is 2.03, 0.1 mm more than in sample of calibrated protectors. The standard deviation is higher as well, having a value of 0.08 mm.

In Fig. 15 is shown a correlation between the dimension A and the switch-off temperature of the toggled protectors. The horizontal axis stands for dimension A and the vertical axis for switch-off temperature in degrees Celsius. The dashed lines mark the tolerance area, horizontal axis defines switch-off temperature tolerances and vertical current tolerances for dimension A. The majority, if not all samples, are away from the line between the two tolerance points, although the tendency is more linear. Many protectors have the dimension A inside the tolerance area, however the switch-off temperature is too high and vice versa.

7. Discussion

For finding the edges by using the AVI system, we have used linear and square polynomial approximation. The superiority of our approach is based on the least mean square approximation method (Eqs. (2)–(4)) that filter the edges. This approach proved to be very useful in our investigation, due to dust particles that are frequently covering the edges. Also, the distances were calculated from math-

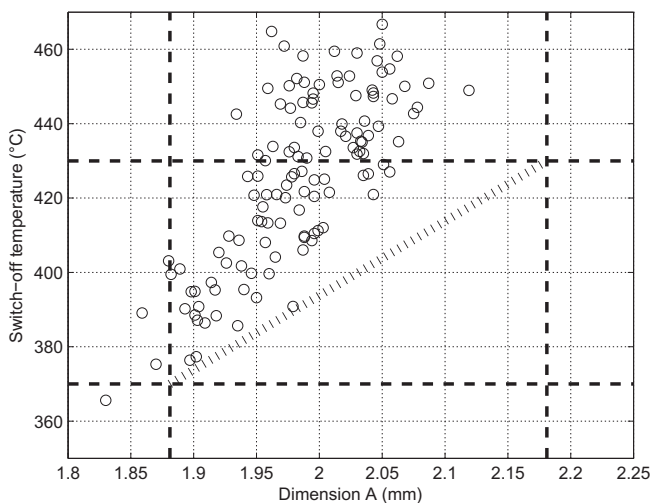


Fig. 15. Sample of 217 non-calibrated protectors: measured dimension A vs. switch-off temperature.

ematical equations of the edges and not directly from number of pixels, which increases the resolution into subpixel region.

The measurements made on five reference protectors with a certified profile projector have proved that measurement accuracy depends on the polynomial order used to transform the number of pixels into metric units. When the linear function is applied, the factor R^2 shows the lowest error on all eight test protectors and does not exceed ± 0.02 mm. With 4th order polynomial, the factor R^2 was maximal, while the error was larger from -0.04 to 0.02 mm.

The detailed analysis of the group of three calibrated protectors showed larger error if linear pixel to metric unit transformation is used. The range of the error is ± 0.02 mm. With 4th order transformation polynomial, the results are much better, having an error of ± 0.01 mm. However, 4th order polynomial is less appropriate for describing other distances. For this reason, the linear transformation is selected to be used in the future, this way distributing the error more equally across the whole measurement area.

Small part of the measurement error can originate from the reference profile projector. Following this analysis it can be specified that measurement uncertainty is within ± 0.01 mm. The parts of the protector having the edges little rounded and also the material that is very shiny are limiting factors for even higher accuracy.

The measurement procedure with the profile projector is identical to the AVI system. The biggest difference is in the lighting conditions. Namely, the AVI system illuminates the background and the profile projector illuminates the foreground, which is causing a difference in determining the edges. However, using the profile projector is the best possible measurement solution, in fact, it is the only possible. The contact distance measurement system is not usable to acquire desired dimensions.

Despite the measurement uncertainty (Eq. (7)) of the profile projector the main source of the measurement error is the AVI system itself or an edge detection algorithm. In some cases the shadows emerge as a consequence of the limit element position. These shadows influence on the offset of the mathematically described edge for a few pixels, with the pixel having a dimension of approximately $4 \mu\text{m}$. The shadows are most frequently present in the area where the edge of the toggle element is determined and also in the area where exact bimetal edge is approximated. These two edges determine the most important distances A and B. Several measurements showed that the error originating from the shadows is in the range of ± 0.02 mm.

The measurement results can be to some order further improved by using the camera with a larger resolution. Some improvement could be also achieved with special and more expensive macro lenses. These would have smaller blurring and higher depth of field as it is presented in this article.

The development originated from need that measured distance A would be obtained contactless as a replacement for slow reference measurements of the switch-off temperatures. Comparative measurements on larger number of protectors did not confirm a direct correlation between distance A and switch-off temperature on both calibrated and non-calibrated groups of protectors (Figs. 12 and 15). When observing the non-calibrated protectors quite linear correlation was recognized. However, the characteristic seem to be steep.

Further analysis and tests using other measurement methods showed that unloaded bimetal has linear bending in the temperature range up to 425°C . In the protector the bimetal is loaded, meaning that linear characteristics end at approximately 300°C . For this reason it is impossible to completely replace slow reference measuring procedure in the oven with dimensional measurements of the protector. The bimetal has too much non-repeatable and non-linear characteristics.

Today the presented AVI system is used in parallel with the slow reference temperature measurement procedure in the laboratory. Before a set of protectors is placed in the oven, all

dimensions are measured with an AVI system. This is important in searching for other correlations, as well as to quickly find false calibrated protectors. In the future, the AVI system use is planned for the production line with the task of eliminating badly calibrated protectors as well as a protector assembly control system.

8. Conclusion

We have developed, calibrated and tested an AVI system for non-contact dimensional measurements of the mechanical system, called the protector. The system consists of a standard monochromatic video camera, standard optics with extension rings and two standard white light emitting diodes (LED). The software enables system calibration, where the user can flexibly transform a number of pixels into metric units. The software also enables flexible measurements, with various tolerance ranges and saving all necessary measured data into a database.

In comparison with the reference profile projector measurement system, the AVI system is much quicker, but also less accurate. The main benefit of presented measurement system is the measurement speed, where all five dimensions are determined in less than a second. With the use of the profile projector measurement system the measurement of these dimensions takes several minutes.

The tests and measurements have shown that the developed measurement system can not be used as replacement of the current temperature measuring method, because the characteristics of the bimetal are not linear and repeatable at higher temperatures, resulting in a wide gap between dimension A and the switch-off temperature of the protector.

The AVI system can be used as a control system in the production for elimination of protectors that have dimensions out of tolerance ranges. Also, the option of saving all measured data can be used in the future for statistic analysis.

Acknowledgment

This work was financially supported by ETA Cerknio Company.

References

- Batchelor, B. G., & Whelan, P. F. (1996). Machine vision systems: Proverbs, principles, prejudices & priorities. In *Proceedings of the SPIE conference on applied machine vision* (Vol. 96, pp. 7–19).
- Chin, R. T., & Harlow, C. A. (1982). Automated visual inspection: A survey. *IEEE Transactions on Pattern Analysis and Machine Intelligence*, 4(6), 557–573.
- Davies, E. R. (2005). *Machine vision: Theory, algorithms, practicalities* (3rd ed.). San Francisco: Elsevier.
- Dom, B. E., & Brecher, V. (1995). *Recent advances in the automatic inspection of integrated circuits for pattern defects, applications*. Springer-Verlag.
- Don Braggins, *Industrial vision application sectors*. <http://homepages.inf.ed.ac.uk/rbf/CVonline/LOCAL_COPIES/ECVNET/Industrial.Vision.html>.
- European Co-operation for Accreditation (1999). *Expressions of the uncertainty of measurements in calibration*, EA-4/02.
- Fang, Y.-C., Liu, T.-K., Macdonald, J., Chou, J.-H., Wu, B.-W., Tsai, H.-L., et al. (2006). Optimizing chromatic aberration calibration using a novel genetic algorithm. *Journal of Modern Optics*, 53(10), 1411–1427.
- Griffin, P. M., & Rene Villalobos, J. (1992). Process of computer vision. *Pattern Recognition*, 24(1), 69–93.
- Haralick, R. M., & Shapiro, L. H. (1991). Glossary of computer vision. *Pattern Recognition*, 24(1), 69–93.
- Ho, C.-S. (1983). Precision of digital vision systems. *IEEE Transactions on Pattern Analysis and Machine Intelligence*, PAMI-5(6), 593–601.
- Hsua, H.-Y., Lina, G. C. I., & Lee, S.-H. (2005). Enhanced image-based coordinate measurement using a super-resolution method. *Robotics and Computer-Integrated Manufacturing*, 21, 579–588.
- International Standard ISO 9445 (2006). *Continuously cold-rolled stainless steel narrow strip, wide strip, plate/sheet and cut lengths. Tolerances on dimensions and form*. Geneva: International Organization for Standardization.
- Miller, J. L., & Friedman, E. (2003). *Photonics rules of thumb, eBook*. McGraw-Hill Professional. p. 418.
- Murase, H., & Nayar, S. K. (1994). Illumination planning for object recognition using parametric eigenspaces. *IEEE Transactions on Pattern Analysis and Machine Intelligence*, 16(12), 1219–1227.
- Newman, T. S., & Jain, A. K. (1995). A survey of automated visual inspection. *Computer Vision and Image Understanding*, 61(2), 231–262.
- Nguyen, H. G. (1995). *A simple method for range finding via laser triangulation*, Technical document 2734. San Diego, CA: Naval Command, Control and Ocean Surveillance Center, RDT&E Division.
- Ravishankar Rao, A. (1996). Future directions in industrial machine vision: Case study of semiconductor manufacturing applications. *Image and Vision Computing*, 14, 3–19.
- Sato, O., Ishikawa, H., Hiraki, M., & Takamasu, K. (2002). The calibration of parallel-CMM: Parallel-coordinate measuring machine. In *Proceeding of the 3rd Euspen international conference* (pp. 573–576). The Netherlands: Eindhoven.
- Tarabanis, K. A., Allen, P. K., & Tsai, R. Y. (1995). A survey of sensor planning in computer vision. *IEEE Transactions on Robotics and Automation*, 11(1), 86–104.